Structure elaboration of isoniazid: Synthesis, in silico molecular docking and antimycobacterial activity of isoniazid–pyrimidine conjugates

Item Type	Article
Authors	Kaur, H;Singh, L;Chibale, K;Singh, K
Citation	Kaur H, Singh L, Chibale K, Singh K. Structure elaboration of isoniazid: synthesis, in silico molecular docking and antimycobacterial activity of isoniazid-pyrimidine conjugates. Mol Divers. 2020 Nov;24(4):949-955. doi: 10.1007/s11030-019-10004-1.
Publisher	Springer Nature
Journal	Molecular Diversity
Rights	Attribution 3.0 United States
Download date	2025-06-12 21:40:51
Item License	http://creativecommons.org/licenses/by/3.0/us/
Link to Item	https://doi.org/10.1007/s11030-019-10004-1

ORIGINAL ARTICLE

Structure elaboration of isoniazid: synthesis, in silico molecular docking and antimycobacterial activity of isoniazid–pyrimidine conjugates

Hardeep Kaur[1] · Lovepreet Singh[1] · Kelly Chibale[2] · Kamaljit Singh[1]

Abstract

Designing small molecule-based new drug candidates through structure modulation of the existing drugs has drawn considerable attention in view of inevitable emergence of resistance. A new series of isoniazid–pyrimidine conjugates were synthesized in good yields and evaluated for antitubercular activity against the H37Rv strain of *Mycobacterium tuberculosis* using the microplate Alamar Blue assay. Structure–anti-TB relationship profile revealed that conjugates **8a** and **8c** bearing a phenyl group at C-6 of pyrimidine scaffold were most active (MIC_{99} 10 μM) and least cytotoxic members of the series. In silico docking of **8a** in the active site of bovine lactoperoxidase as well as a cytochrome C peroxidase mutant N184R Y36A revealed favorable interactions similar to the heme enzyme catalase peroxidase (KatG) that activates isoniazid. This investigation suggests a rationale for further work on this promising series of antitubercular agents.

Graphic abstract

MIC_{99} 10 μM ($H_{37}R_V$)
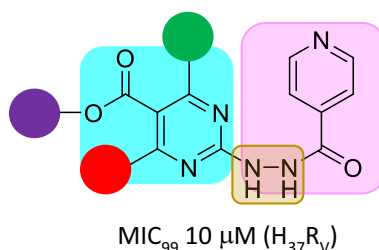
Keywords Isoniazid · Pyrimidine · Conjugates · Tuberculosis · Drug resistance · Molecular docking · ADME

Hardeep Kaur and Lovepreet Singh have contributed equally to this work.

✉ Kamaljit Singh
  kamaljit.chem@gndu.ac.in

1 Department of Chemistry, UGC Centre of Advance Study-II, Guru Nanak Dev University, Amritsar 143 005, India

2 South African Medical Research Council Drug Discovery and Development Research Unit, Department of Chemistry and Institute of Infectious Disease and Molecular Medicine, University of Cape Town, Rondebosch 701, South Africa

Abbreviations

MABA	Microplate Alamar Blue assay
WHO	World Health Organization
SDG	Sustainable development goals
INH	Isoniazid
RIF	Rifampicin
PZA	Pyrazinamide
EMB	Ethambutol
PPE	Polyphosphate ester
KatG	Heme (ferric) enzyme catalase peroxidase
MTT	3-(4,5-Dimethylthiazol-2-yl)-2,5-diphenyltetra-zoliumbromide
InhA	2-*trans*-enoyl-acyl carrier protein reductase
ADME	Adsorption, distribution, metabolism, excretion

Multidrug-resistant diseases constitute a public health crisis and a dastardly curse on humanity as the resistance to the most first-line drugs poses a serious challenge to the health security, especially of the weaker section of population [1]. The situation exacerbates when the disease is communicable and is asymptomatic during the initial phase, which often delays onset of active treatment only to result in transmission to others [2]. Tuberculosis (TB) is a contagious, infectious disease caused by bacteria (*Mycobacterium tuberculosis*) and is one of the major causes of death worldwide [3, 4]. In 2017 only, at least 1.6 million (including 0.3 million HIV positive) people died from this disease. As per the estimate of the World Health Organization (WHO) [5], there were 558,000 new cases of multidrug-resistant TB (MDR-TB) with resistance to the most effective rifampicin. While "end of TB" as an epidemic remains an aspiration, the initiatives of the sustainable development goals (SDG) to end TB by 2030 needs to be supported to make it a reality [6, 7]. In this direction, repurposing of existing drugs [8], derivatization of the existing drugs [9] and screening libraries of new chemical entities [10] to find novel compounds, which could act through different mechanisms against the TB bacterium, and design of new drugs [11, 12] that can shorten and improve TB treatment are the mainstay approaches used for finding drug leads. Molecular hybrids [13, 14], obtained by covalent linking of two different pharmacophores, offer advantages in terms of solubility and efficiency in formulation/delivery and circumvent limitations of single drug or combination therapy. Such drugs which promise dual mode of action are expected to avoid/delay emergence of drug resistance.

Isoniazid (INH **1**, Fig. 1) [15] is one of the most effective first-line anti-TB drugs, which is generally administered in combination with rifampicin, pyrazinamide or ethambutol. However, undesirable drug interactions in the combination,
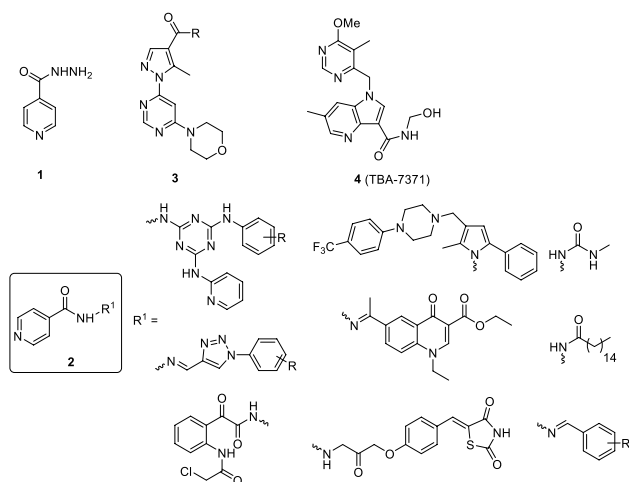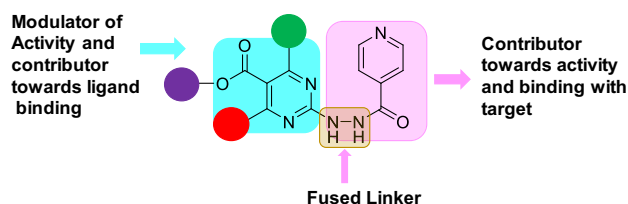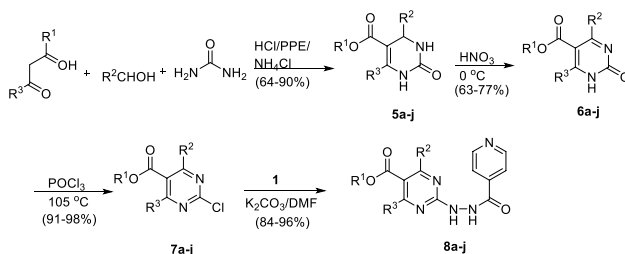

Fig. 2 Design strategy of INH–pyrimidine conjugates and structure–property indicators

mismatched pharmacokinetics and pharmacodynamics, length of the therapy and side effects such as hepatotoxicity constitute some of the key limitations [16, 17]. However, the use of anti-TB molecular hybrids [18] (**2**, Fig. 1) based on INH as one of the hybrid partners has been reported to not only exhibit good anti-TB activity, but also circumvent several limitations of the combination therapy. Meanwhile, pyrimidines have reasonably broad spectrum of pharmacological activities such as antimalarial [19–23], anti-AIDS [24, 25], antinociceptive [26, 27], antifungal [28, 29], anticancer [30, 31] as well as antitubercular [32–34]. Some of the molecular hybrids using pyridine sub-unit (**3,4**) [35, 36] with good anti-TB activity are shown in Fig. 1. We hypothesized elaborating structure of INH by linking INH with pyrimidines to obtain small molecular conjugates would not only provide new molecular hybrids, but also provide an opportunity to evaluate their structure-dependent anti-TB activity. Using the design strategy shown in Fig. 2, we synthesized a series of compounds and evaluated their anti-TB activity against H37Rv strains of *M. tuberculosis* using the microplate Alamar Blue assay (MABA) and deduced their structure–activity relationship profile. Additionally, we have assayed the cytotoxicity of selected hybrids against the mammalian Vero cell line. We also performed in silico molecular docking of the most active compound in the active sites of bovine lactoperoxidase (PDB ID: 3I6N) as well as a cytochrome C peroxidase (PDB ID: 2V2E) mutant N184R Y36A to understand their binding patterns.

The INH–pyrimidine conjugates were synthesized using the protocol outlined in Scheme 1. The precursor alkyl 6-methyl/phenyl-2-oxo-4-substituted-1,2,3,4-tetrahydropy-


Fig. 1 Structures of isoniazid (INH, **1**) and molecular hybrids: based on INH (**2**), and pyrimidine core (**3,4**)

Scheme 1 Synthesis of INH–pyrimidine conjugates **8a–j**

Table 1 Structure of **5–8**, in vitro antitubercular activity and cytotoxicity of INH–pyrimidine conjugates **8a–j** and reference drugs

Entry	Structure (Scheme 1)				8a–j				
	5–8	R^1	R^2	R^3	Yield (%)	CLogP[a]	MIC$_{99}$ (µM)[b,c]	IC$_{50}$ (µM)[b,d]	SI[e]
1	a	Me	Ph	Me	88	1.55	10	> 275	> 27.5
2	b	Et	Ph	Me	92	2.08	40	> 265	> 6.6
3	c	iso-Pr	Ph	Me	84	2.39	10	> 255	> 25.5
4	d	Et	Me	Ph	90	2.08	> 160	nd	nd
5	e	Me	Me	Me	95	0.04	> 160	nd	nd
6	f	Et	Me	Me	96	0.48	40	nd	nd
7	g	Et	p-F(C_6H_4)	Me	95	2.23	40	nd	nd
8	h	Et	p-MeO(C_6H_4)	Me	90	2.12	> 160	> 245	> 1.53
9	i	iso-Pr	m-NO$_2$(C_6H_4)	Me	86	2.14	40	nd	nd
10	j	iso-Pr	p-NO$_2$(C_6H_4)	Me	92	2.14	80	nd	nd
11	1 (Figure 1)				–	− 0.66	0.1423	729	5123
12	RIF[f]	–			–	− 0.67	0.009	–	–
13	9[f]	–			–	− 5.2	1.340	–	–
14	10[f]	–			–	–	–	0.12	–

[a]Calculated from Chem draw Ultra 11.0; [b]Mean of three observations; [c]MIC$_{99}$ (µM) at day 14 in GAST/Fe with H37Rv (microplate Alamar Blue); [d]50% cytotoxic concentration (Vero cell lines); [e]SI is the ratio of cytotoxicity (IC$_{50}$ in µM) to MIC$_{99}$ (in vitro activity against *M. tuberculosis* H37Rv) expressed in µM; nd—not determined; [f]See below

Rifampicin (RIF)   **9** (Kanamycin)   **10** (Emetine)
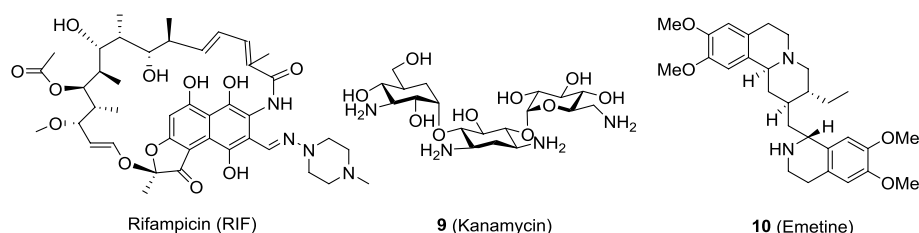
rimidine-5-carboxylates **5a–j** were prepared through HCl or polyphosphate ester (PPE)-catalyzed three-component Biginelli condensation [37–43] of an alkyl acetoacetic ester, urea and appropriate aldehyde in anhydrous EtOH. Oxidation of **5a–j** using nitric acid (aqueous 70% *v/v*) readily furnished the corresponding alkyl 6-methyl/phenyl-2-oxo-4-substituted-1,2-dihydropyrimidine-5-carboxylates **6a–j**. Chlorination of **6a–j** with phosphorous oxychloride (POCl$_3$) yielded the corresponding alkyl 2-chloro-4-methyl/phenyl-6-substituted pyrimidine-5-carboxylate **7a–j**. Nucleophilic substitution reaction of **7a–j** with **1** (prepared from the commercially available 4-cyanopyridine and hydrazine hydrate) gave alkyl 4-methyl/phenyl-2-(2-isonicotinoylhydrazinyl)-6-substituted pyrimidine-5-carboxylates **8a–j** (INH–pyrimidine conjugates) in 84–96% yield (Table 1). Structures of **5–8** were unambiguously established on the basis of spectral (^{1}H NMR, ^{13}C NMR, MS, FTIR) data as well as microanalytical analysis (See Supporting Information).

Isoniazid **1** exerts its anti-TB activity by inhibiting the synthesis of mycolic acid, which is one of the essential chemical pathways for the formation of the mycobacterial cell wall in *M. tuberculosis* bacterium. In the current design of conjugates (Fig. 2), it was expected that the structure modification of **1** may influence the physicochemical properties such as lipophilicity and/or diffusion through the lipid-rich bacterial cell wall and modulate the binding of these conjugates in the binding domain of biological targets and exert anti-TB activity. The designed INH–pyrimidine conjugates **8a–j** indeed showed high lipophilicity (cLogP: 0.04–2.39; Table 1) relative to INH as well as favorable binding interactions similar to heme (ferric) enzyme catalase peroxidase (KatG) endogenous to *M. tuberculosis*.

Conjugates **8a–j** were tested for in vitro antitubercular activity against H$_{37}$Rv strains of *M. tuberculosis* using the MABA assay and depicted (Table 1) good to moderate activity in µM range, although the activity was less than the standard drugs viz. **1**, rifampicin (RIF) and kanamycin. Correlating anti-TB activity with structure of these conjugates revealed interesting trends. Replacing the C-5 ethyl ester of **8b** [MIC$_{99}$ 40 µM] with methyl (**8a**) or isopropyl ester (**8c**) [**8a** = **8c**: MIC$_{99}$ 10 µM] (Entries 1–3, Table 1) led to an increase in antitubercular activity. Similarly, when the

phenyl substituent at the C-6 position of the pyrimidine core of the compounds **8a/8b** was replaced with a methyl group, while a decrease in antitubercular activity of the resultant derivative **8e** was observed (Entry 5, Table 1) compared to the former, the activity of **8f** was similar to that of **8b**. Switching the substituents at C-4 and C-6 positions of **8d** to make **8b** showed a fourfold increase in activity (Table 1). We further incorporated differently substituted (*p*-fluoro/*p*-methoxy/*m*-/*p*-nitro) aryl substituents at C-6 position of the pyrimidine ring (Table 1). Thus, compared to **8b**, introduction of a *p*-fluoro group in **8g** (Entry 7, Table 1) did not show change in activity, a *p*-methoxy substituent led to a fourfold decrease (Table 1). Likewise, compared to **8c**, one of the most active members of the series, introducing a *m*-nitrophenyl (**8i**) or *p*-nitro phenyl (**8j**) substituents at C-6 position of the pyrimidine core resulted in, respectively, two- and fourfold decrease in the antitubercular activity, while their activity was significantly superior to **8h** (Entry 8, Table 1). Among the nitro-substituted conjugates, the *m*-nitrophenyl-substituted **8i** (MIC_{99} 40 µM) was twofold more active than the corresponding *p*-nitrophenyl-substituted **8j** (MIC_{99} 80 µM). This brief structure–antitubercular activity profile suggested that the variation of substituents at C-4 and C-6 positions of pyrimidine moiety modulates the antitubercular activity of these conjugates. Cytotoxicity of selected compounds was assayed against mammalian Vero cell line using 3-(4,5-dimethylthiazol-2-yl)-2,5-diphenyltetrazoliumbromide (MTT)-assay. The IC_{50} values were in µM concentration and are summarized in Table 1. The cytotoxicity data revealed that the most potent compounds (**8a** and **8c**) are fairly non-toxic (Table 1) and also less cytotoxic than reference drug Emetine, although the cytotoxicity of the hybrids was greater than **1**. The ratios between cytotoxicity (IC_{50} in µM) and in vitro antitubercular activity (MIC in µM) enabled the determination of selectivity index (SI). The compounds that exhibited SI values greater than 10 are considered non-toxic. Comparison of the selectivity index of potent compounds also suggested that hybrids **8a** and **8c** had higher SI values and were less cytotoxic. Thus, although none of these conjugates was more active than the parent **1**, more structure diversification may lead to the refinement of the molecular design and the attendant antitubercular activity.

The prodrug INH is activated by the heme (ferric) enzyme catalase peroxidase (KatG) endogenous to *M. tuberculosis*. Specifically, upon activation with KatG, INH is transformed into a potent antimycobacterial intermediate, which in combination with NADH forms an adduct [44], which inhibits inhA (2-*trans*-enoyl-acyl carrier protein reductase) of *M. tuberculosis*. This leads to inhibition of synthesis of mycolic acid, a major lipid of the bacterial cell wall. However, the mechanism of activation is poorly understood, partly because the binding interaction has not been properly established. At the same time, mutation in
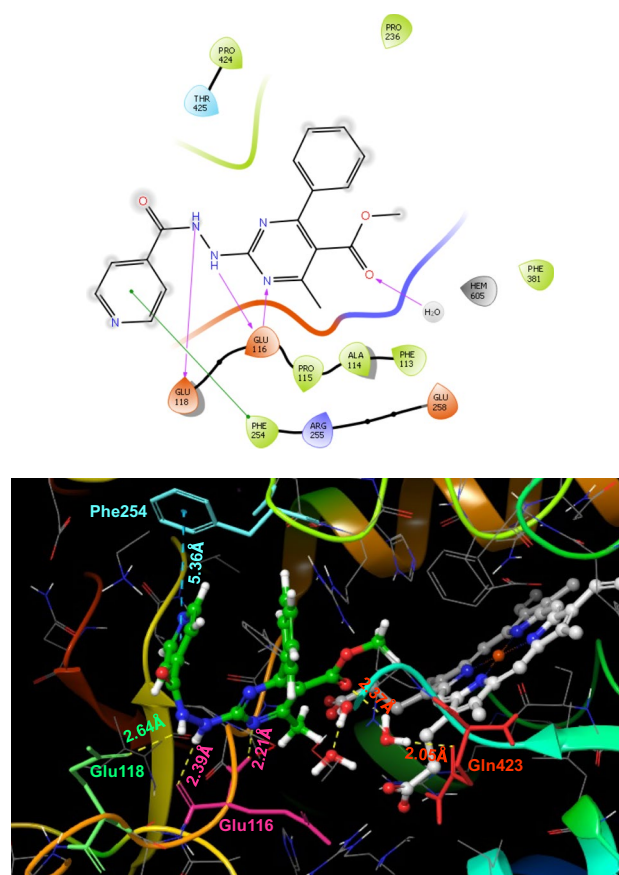

Fig. 3 Two- and three-dimensional docking poses of compound **8a** showing the interactions in the binding sites of bovine lactoperoxidase (PDB ID: 3I6N)

KatG of *M. tuberculosis* is reported to be a major factor of INH resistance. Consequently, most drug-resistant *M. tuberculosis* strains are resistant to INH. Literature reports [45] that INH is activated by mammalian lactoperoxidase and *mycobacterium* KatG. Consequently, in this study, using Schrodinger, LLC, New York, NY, 2019, we have conducted docking studies of the most active member **8a** of the series with bovine lactoperoxidase (PDB ID: 3I6N) as well as a cytochrome C peroxidase (PDB ID: 2V2E) mutant N184R Y36A, as the active sites of the latter are very much similar to KatG and are capable of activating INH. The pyrimidine ring of the hybrid partner contributes in making π-stacking interactions with Phe254 (ring-to-ring distance 5.36 Å). The N2-H (next to CO) of the hydrazide moiety of INH unit binds through hydrogen bonding to Glu118 (Glu118···H–N2: 2.64 Å) (Fig. 3), while N3–H of the hydrazide is hydrogen bonded to Glu116 (Glu116-O···H–N3: 2.39 Å). Likewise, N3 of the pyrimidine ring also makes hydrogen bonding interaction with Glu116 (Glu116-O···H–N3-Pyr: 2.21 Å). The ester carbonyl oxygen atom is hydrogen bonded with a molecule of water (2.37 Å), the latter is further bonded,
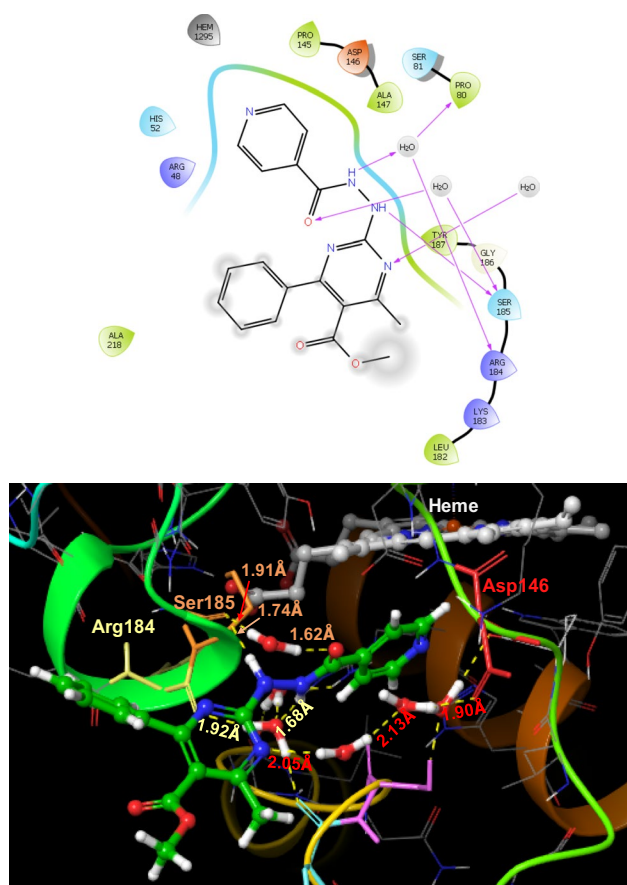
Fig. 4 Two- and three-dimensional docking poses of compound **8a** showing the interactions in the binding sites of cytochrome C peroxidase (PDB ID: 2V2E) mutant N184R Y36A

through hydrogen bonding with Gln423 (2.05 Å) residue. Compared to the docking of pristine INH in the binding pocket of 3I6N (Fig. SI), through π-stacking interactions with Arg255A and hydrogen bonding of the hydrazide NH with Gln423A, the hybrid **8a** shows additional interactions of the hybrid partner (pyrimidine unit) with the ligand binding sites as projected in Fig. 2.

The docking of **8a** into the active site of the cytochrome C peroxidase (PDB ID: 2V2E) revealed binding of N3H of the hydrazide moiety with Ser185 (Ser185-O···H–N3: 1.74 Å). The N2H of **8a** is bonded to a water molecule (N2H···H–OH: 1.68 Å), which in turn is bound to Arg184 (Arg184-O···H–OH: 1.92 Å). Interestingly, while the carbonyl oxygen atom of INH makes interaction with Phe254 (Phe254-H···O=C), in the case of **8a**, its binding with Ser185 is intercepted by a water molecule (C=O···H–OH: 1.62 Å), which acts as a bridge to bind the oxygen atoms of both Ser185 (Ser185-O···H–OH: 1.91 Å), as well as carbonyl group of **8a** (Fig. 4). The SPG scores of the docking of **8a** in the active sites of the bovine lactoperoxidase (PDB ID: 3I6N) and cytochrome C peroxidase (PDB ID: 2V2E) were

−4.348 and −5.732, respectively, while the Glide energies were −27.699 and −23.605 kcal/mol, respectively.

Prediction of ADME parameters for all the members of this series of hybrids was performed, and the results are presented in Table S1 of Supporting Information. Except QPlogHERG descriptor (prediction for HERG-K+ channel inhibition) and QPPMDCK for **8i** and **8j**, all other ADME parameters were found to lie within the acceptable range.

In summary, a new series of INH–pyrimidine conjugates were prepared as potential antitubercular conjugates against H37Rv strains of *M. tuberculosis*. The compounds depicted structure-dependent antitubercular activity. Two conjugates, **8a** and **8c**, were identified as the most active of this series. However, none of these compounds was more active than isoniazid, and thus, more structure optimization is required for these new conjugates. Cytotoxicity of selected compounds was assayed against mammalian Vero cell line, and the most active members were less cytotoxic than emetine used as the reference standard.

Author Contributions The manuscript was written through contributions of all authors. All authors have given approval to the final version of the manuscript.

References

1. Tanwar J, Das S, Fatima Z, Hameed S (2014) Multidrug resistance: an emerging crisis. Interdiscip Perspect Infect Dis 2014:541340
2. Monge-Maillo B, Lopez-Velez R, Norman FF, Ferrere-Gonzalez F, Martınez-Perez A, Perez-Molina JA (2015) Screening of imported infectious diseases among asymptomatic sub-Saharan African and Latin American immigrants: a public health challenge. Am J Trop Med Hyg 92:848–856
3. Sakamoto K (2012) The pathology of *Mycobacterium tuberculosis* infection. Vet Pathol 49:423–439
4. Russel DG (2001) *Mycobacterium tuberculosis*: here today, and here tomorrow. Nat Rev Mol Cell Biol 2:569–577
5. Global Tuberculosis report 2018, WHO
6. Uplekar M, Weil D, Lonnroth K, Jaramillo E, Lienhardt C, Dias HM, Falzon D, Floyd K, Gargioni G, Getahun H, Gilpin C, Glaziou P, Grzemska M, Mirzayev F, Nakatani H, Raviglione M (2015) WHO's new end TB strategy. Lancet 385:1799–1801
7. Lonnarth K, Raviglione M (2016) The WHO's new end TB strategy in the post-2015 era of the sustainable development goals. Trans R Soc Trop Med Hyg 110:148–150
8. Pushpakom S, Iorio F, Eyers PA, Escott KJ, Hopper S, Wells A, Doig A, Guilliams T, Latimer J, McNamee C, Norris A, Sanseau P, Cavalla D, Pirmohamed M (2019) Drug repurposing: progress, challenges and recommendations. Nat Rev Drug Discov 18:41–58

9. Knowles DJ (1997) New strategies for antibacterial drug design. Trends Microbiol 5:379

10. Broach JR, Thorner J (1996) High-throughput screening for drug discovery. Nature 384:14–16

11. Gualano G, Capone S, Mattelli A, Palmien F (2016) New antituberculosis drugs: from clinical trial to programmatic use. Infect Dis Rep 8:6569

12. Zumla A, Chakaya J, Centis R, D'Ambrosio L, Mwaba P, Bates M, Kapata N, Nyirenda T, Chanda D, Mfinanga S, Hoelscher M, Maeurer M, Migliori GB (2015) Tuberculosis treatment and management–an update on treatment regimens, trials, new drugs, and adjunct therapies. Lancet Respir Med 3:220–234

13. Meunier B (2008) Hybrid molecules with a dual mode of action: dream or reality? Acc Chem Res 41:69–77

14. Muregi FW, Ishih A (2010) Next-generation antimalarial drugs: hybrid molecules as a new strategy in drug design. Drug Dev Res 71:20–32

15. Bass Jr JB, Farer LS, Hopewell PC, O'Brien R, Jacobs RF, Ruben F, Snider Jr DE, Thornton GS (1994) Treatment of tuberculosis and tuberculosis infection in adults and children. American Thoracic Society and The Centers for Disease Control and Prevention. Am J Respir Crit Care Med 149:1359–1374

16. Srivastava S, Pasipanodya J, Meek C, Leff R, Gumbo T (2011) Multidrug-resistant tuberculosis not due to noncompliance but to between-patient pharmacokinetic variability. J Infect Dis 204:1951–1959

17. Singh M, Sasi P, Rai G, Gupta VH, Amarapurkar D, Wangikar PP (2011) Studies on toxicity of antitubercular drugs namely isoniazid, rifampicin, and pyrazinamide in an in vitro model of HepG2 cell line. Med Chem Res 20:1611–1615

18. Hu Y-Q, Zhang S, Zhao F, Gao C, Feng L-S, Lv Z-S, Xu Z, Wu X (2017) Isoniazid derivatives and their anti-tubercular activity. Eur J Med Chem 133:255–267

19. Tripathi M, Taylor D, Khan SI, Tekwani BL, Ponnan P, Das US, Velpandian T, Rawat DS (2019) Hybridization of fluoro-amodiaquine (FAQ) with pyrimidines: synthesis and antimalarial efficacy of FAQ-pyrimidines. ACS Med Chem Lett 10:714–719

20. Singh K, Kaur T (2016) Pyrimidine-based antimalarials: design strategies and antiplasmodial effects. Med Chem Commun 7:749–768

21. Kaur H, Chibale K, Smith P, de Kock C, Singh K (2015) Synthesis, antiplasmodial activity and mechanistic studies of pyrimidine-5-carbonitrile and quinoline hybrids. Eur J Med Chem 101:52–62

22. Kaur H, Machado M, Chibale K, Prudêncio M, Singh K (2015) Primaquine–pyrimidine hybrids: synthesis and dual-stage antiplasmodial activity. Eur J Med Chem 101:266–273

23. Singh K, Kaur H, Smith P, de Kock C, Chibale K, Balzarini J (2014) Quinoline-pyrimidine hybrids: synthesis, antiplasmodial activity, SAR, and mode of action studies. J Med Chem 57:435–448

24. Romeo R, Iannazzo D, Veltri L, Gabriele B, Macchi B, Frezza C, Merlo FM, Giofre SV (2019) Pyrimidine 2,4-diones in the design of new HIV RT inhibitors. Molecules 24:1718

25. Okazaki S, Mizuhara T, Shimura K, Murayama H, Ohno H, Oishi S, Matsuoka M, Fujii N (2015) Identification of anti-HIV agents with a novel benzo[4,5]isothiazolo[2,3-a]pyrimidine scaffold. Bioorg Med Chem 23:1447–1452

26. Varano F, Catarzi D, Vincenzi F, Betti M, Falsini M, Ravani A, Borea PA, Colotta V, Varani K (2016) Design, synthesis, and pharmacological characterization of 2-(2-Furanyl)thiazolo[5,4-d]pyrimidine-5,7-diamine derivatives: new highly potent A2A adenosine receptor inverse agonists with antinociceptive activity. J Med Chem 59:10564–10576

27. Bookser BC, Ugarkar BG, Matelich MC, Lemus RH, Allan M, Tsuchiya M, Nakane M, Nagahisa A, Wiesner JB, Erion MD (2005) Adenosine kinase inhibitors. 6. Synthesis, water solubility, and antinociceptive activity of 5-phenyl-7-(5-deoxy-β-d-ribofuranosyl)pyrrolo[2,3-d]pyrimidines substituted at C4 with glycinamides and related compounds. J Med Chem 48:7808–7820

28. Wu W, Chen M, Wang R, Tu H, Yang M, Ouyang G (2019) Novel pyrimidine derivatives containing an amide moiety: design, synthesis, and antifungal activity. Chem Pap 73:719–729

29. Maddila S, Gorle S, Seshadri N, Lavanya P, Jonnalagadda SB (2016) Synthesis, antibacterial and antifungal activity of novel benzothiazole pyrimidine derivatives. Arab J Chem 9:681–687

30. Ma Z, Gao G, Fang K, Sun H (2019) Development of novel anticancer agents with a scaffold of tetrahydropyrido[4,3-d]pyrimidine-2,4-dione. ACS Med Chem Lett 10:191–195

31. Gokhale N, Dalimba U, Kums M (2017) Facile synthesis of indole-pyrimidine hybrids and evaluation of their anticancer and antimicrobial activity. J Saudi Chem Soc 21:761–775

32. Liu P, Yang Y, Tang Y, Yang T, Liu Z, Zhang T, Luo Y (2019) Design and synthesis of novel pyrimidine derivatives as potent antitubercular agents. Eur J Med Chem 163:169–182

33. Ke S, Shi L, Zhang Z, Yang Z (2017) Steroidal[17,16-d]pyrimidines derived from dehydroepiandrosterone: a convenient synthesis, antiproliferation activity, structure-activity relationships, and role of heterocyclic moiety. Sci Rep 7:44439

34. Singh K, Singh K, Wan B, Franzblau S, Chibale K, Balzarini J (2011) Facile transformation of Biginelli pyrimidin-2(1H)-ones to pyrimidines. In vitro evaluation as inhibitors of *Mycobacterium tuberculosis* and modulators of cytostatic activity. Eur J Med Chem 46:2290–2294

35. Vekariya MK, Vekariya RH, Patel KD, Raval NP, Shah PU, Rajani DP, Shah NK (2018) Pyrimidine-pyrazole hybrids as morpholino-pyrimidine-based pyrazole carboxamides: synthesis, characterisation, docking, ADMET study and biological evaluation. ChemistrySelect 3:6998–7008

36. Chatterji M, Shandil R, Manjunatha MR, Solapure S, Ramachandran V, Kumar N, Saralaya R, Panduga V, Reddy J, Prabhakar KR, Sharma S, Sadler C, Cooper CB, Mdluli K, Iyer PS, Narayanan S, Shirude PS (2014) 1, 4-Azaindole, a potential drug candidate for treatment of tuberculosis. Antimicrob Agents Chemother 58:5325–5331

37. Biginelli P, Gazz P (1893) Synthesis of 3,4-Dihydropyrimidin-2(1H)-Ones. Chim Ital 23:360–416

38. Singh K (2012) Biginelli condensation: synthesis and structure diversification of 3,4-dihydropyrimidin-2(1H)-one derivatives. In: Katritzky AR (ed) Advances in heterocyclic chemistry, vol 105. Academic Press, Cambridge, pp 223–308

39. Kappe CO (2003) The generation of dihydropyrimidine libraries utilizing Biginelli multicomponent chemistry. QSAR Comb Sci 22:630–645

40. Falsone FS, Kappe CO (2001) The Biginelli dihydropyrimidone synthesis using polyphosphate ester as a mild and efficient cyclo-condensation/dehydration reagent. Arkivoc 2:122–134

41. Shaabani A, Bazgir A, Teimouri F (2003) Ammonium chloride-catalyzed one-pot synthesis of 3, 4-dihydropyrimidin-2-(1H)-ones under solvent-free conditions. Tetrahedron Lett 44:857–859

42. Strohmeier GA, Kappe CO (2002) Rapid parallel synthesis of polymer-bound enones utilizing microwave-assisted solid-phase chemistry. J Comb Chem 4:154–161

43. Puchala A, Belaj F, Bergman J, Kappe CO (2001) On the reaction of 3,4-dihydropyrimidones with nitric acid. Preparation and x–ray structure analysis of a stable nitrolic acid. J Heterocycl Chem 38:1345–1352

44. Metcalfe C, Macdonald IK, Murphy EJ, Brown KA, Raven EL, Moody PCE (2008) The tuberculosis prodrug isoniazid bound to activating peroxidases. J Biol Chem 283:6193–6200

45. Singh AK, Kumar RP, Pandey N, Singh N, Sinha M, Bhushan A, Kaur P, Sharma S, Singh TP (2010) Mode of binding of the tuberculosis prodrug isoniazid to heme peroxidases: binding studies and crystal structure of bovine lactoperoxidase with isoniazid at 2.7 A resolution. J Biol Chem 285:1569–1576